Front. Struct. Civ. Eng. 2024, 18(4): 551–567
https://doi.org/10.1007/s11709-024-1091-1

RESEARCH ARTICLE

Engineering punching shear strength of flat slabs predicted by nature-inspired metaheuristic optimized regression system

Dinh-Nhat TRUONG[a], Van-Lan TO[a], Gia Toai TRUONG[b*], Hyoun-Seung JANG[c*]

[a] *Department of Civil Engineering, University of Architecture Ho Chi Minh City, Ho Chi Minh City 700000, Vietnam*
[b] *Faculty of Civil Engineering and Technology, Dong A University, Da Nang City 550000, Vietnam*
[c] *School of Architecture, Seoul National University of Science and Technology, Seoul 01811, Republic of Korea*
[*] *Corresponding authors. E-mails: toaitg@donga.edu.vn; jang@seoultech.ac.kr*

© The Author(s) 2024. This article is published with open access at link.springer.com and journal.hep.com.cn

ABSTRACT Reinforced concrete (RC) flat slabs, a popular choice in construction due to their flexibility, are susceptible to sudden and brittle punching shear failure. Existing design methods often exhibit significant bias and variability. Accurate estimation of punching shear strength in RC flat slabs is crucial for effective concrete structure design and management. This study introduces a novel computation method, the jellyfish-least square support vector machine (JS-LSSVR) hybrid model, to predict punching shear strength. By combining machine learning (LSSVR) with jellyfish swarm (JS) intelligence, this hybrid model ensures precise and reliable predictions. The model's development utilizes a real-world experimental data set. Comparison with seven established optimizers, including artificial bee colony (ABC), differential evolution (DE), genetic algorithm (GA), and others, as well as existing machine learning (ML)-based models and design codes, validates the superiority of the JS-LSSVR hybrid model. This innovative approach significantly enhances prediction accuracy, providing valuable support for civil engineers in estimating RC flat slab punching shear strength.

KEYWORDS punching shear strength, reinforced concrete flat slabs, machine learning, jellyfish search, support vector machine

1 Introduction

In recent years, one of the most widely adopted slab systems in building construction has been reinforced concrete (RC) flat slabs. The popularity of flat slabs can be attributed to their straightforward, swift, and cost-effective construction, involving uncomplicated sheathing and reinforcement layouts [1]. Furthermore, the use of RC flat slabs offers architectural flexibility and increased room height due to their low construction height, leading to time and cost savings [2]. However, the safety of the structure hinges on the punching shear capacity around the supporting columns during the design of RC flat slabs [3]. This is crucial because punching shear represents a brittle failure mechanism that can result in a sudden and complete collapse of the entire structure without warning [4]. Consequently, researchers continue to conduct extensive investigations in this area [5,6].

Numerous experimental studies have been conducted to assess the performance of RC flat slabs. Researchers such as Theodorakopoulos and Swamy [7], Metwally et al. [8], Birkle and Dilger [9], Rizk et al. [10], Shatarat and Salma [11], and Hoang and Pop [12] have carried out tests on RC flat slabs to investigate various geometric and mechanical parameters affecting punching shear failure. These studies have not only offered insights into the behavior of RC flat slabs under punching shear forces, but also created a valuable data source for researchers to develop and validate upcoming models.

Drawing from a comprehensive database compiled from existing literature, an increasing number of researchers have developed both empirical and theoretical

Article history: Received Aug 22, 2023; Accepted Nov 18, 2023

models to predict the punching shear strength of RC flat slabs. Several approaches have been proposed, including the strut-and-tie models for slab-column connections that facilitate clear force distribution in rotation-symmetric cases, as suggested by Alexander and Simmonds [13]. Huang et al. [14] devised a bending-shearing critical crack method based on crack image and load-deformation relationships derived from test data, enabling the prediction of punching shear strength in RC slab-column connections. Elshafey et al. [15] formulated two simplified empirical equations using 244 sets of test data, demonstrating their good fit with the compiled database. Deifalla [16] developed a mechanically sound model for concrete slabs subjected to combined punching shear and in-plane tensile forces, validated with 52 test cases.

Kueres et al. [17] introduced a uniform design method by enhancing Eurocode 2 for predicting the punching shear strength of both flat slabs and column bases. Moreover, Park et al. [18] assessed the punching shear strength of RC slab-column connections based on the failure mechanism of concrete in the compression zone, utilizing Rankine's failure criteria for the interaction between compressive normal and shear stresses. Numerous formulas arising from these studies have been incorporated into practical design codes, such as ACI 318-19 [19], Eurocode 2 [20], and BS 8110 [21].

In recent years, machine learning (ML) techniques have gained popularity and proven to be effective in solving various problems in structural engineering [22–28], particularly in the context of RC flat slabs and slab-column connections. For instance, Choi et al. [29] developed a fuzzy model to predict the punching shear strength of interior slab-column connections based on a data set comprising 178 samples. Erdem [30] created an artificial neural network (ANN) model using 294 calculated data points to estimate the ultimate moment capacity of RC slabs exposed to fire. Additionally, Elshafey et al. [15], Akbarpour and Akbarpour [31], Chetchotisak et al. [32], and Tran and Kim [33] developed separate ANN models for predicting the punching shear strength of RC flat slabs. Each of these models was trained on a different data set, consisting of 244, 189, 342, and 218 data points, respectively. The models yielded varied prediction results due to differences in their training data.

Mangalathu et al. [34] conducted a study aimed at establishing a prediction model for the punching shear strength of RC flat slabs using various regression models. The results obtained indicated that the XGBoost model demonstrated superior prediction performance compared to other ML models. In a separate study, Wu and Zhou [35] employed a hybrid particle swarm optimization-support vector regression (PSO-SVR) model, which combines SVR and the PSO algorithm, to predict the punching shear strength of two-way RC slabs. This prediction was based on 218 data sets with six design parameters as input variables. They discovered that the optimized PSO-SVR model outperformed the original SVR model, exhibiting a higher correlation coefficient (R) and smaller error indices. Both studies [34,35] utilized the well-known shapely additive explanation method to conduct feature importance and sensitivity analyses, analyzing the effect of design parameters on punching shear strength. It was found that the effective depth of the slab had the most significant impact on predicting the punching shear strength of RC flat slabs.

There are various optimization methods, including gradient-based techniques such as the method of moving asymptotes [36–38], and gradient-free techniques such as genetic algorithms (GA) and jellyfish swarm (JS). Meta-heuristic optimization algorithms, a type of gradient-free optimization technique, are becoming increasingly popular for solving complex problems in diverse domains. Several factors contribute to their growing popularity. First, they rely on simple concepts and are easy to implement. Secondly, they do not require information about the gradient of the objective function. Thirdly, they can bypass local minima. Lastly, they can be utilized to solve a wide range of problems in different fields. As a result, the JS algorithm, a meta-heuristic optimization, is employed in this study to optimize ML parameters [39].

Thus, we propose a novel hybrid ML-based model, named jellyfish-least square support vector machine (JS-LSSVR), to accurately predict the punching shear strength of RC flat slabs under concentric loads, without the presence of transverse reinforcement. The JS-LSSVR hybrid model optimizes the hyperparameters of LSSVR using a swarm intelligence algorithm, ensuring reliable and precise predictions. A comprehensive literature review revealed that the JS-LSSVR method is introduced for the first time in predicting the punching shear strength of RC flat slabs.

The proposed model undergoes training and testing using 511 test specimens gathered from previous studies. A 10-fold cross-validation technique is employed to minimize bias and enhance prediction consistency. The optimization performance of the Jellyfish Search (JS) algorithm is compared with seven other well-known optimizers, including the artificial bee colony (ABC) algorithm, differential evolution (DE) algorithm, GA, gray wolf optimization (GWO), PSO, teaching learning-based optimization (TLBO), and whale optimization (WO) algorithm. Finally, the accuracy and prediction performance of the hybrid model are thoroughly examined and compared with existing ML-based models and current design codes to evaluate its efficiency.

2 Methodology

2.1 Least square support vector regression

Proposed by Suykens et al. [40], LSSVR theory assumes

that the data set $S=\{(x_1,y_1),(x_2,y_2),\ldots,(x_n,y_n)\}$ can be represented as a nonlinear function and a decision function, given in Eq. (1).

$$y(x)=\omega^{T}\phi(x)+b, \tag{1}$$

where $x\in\mathbb{R}^n, y\in\mathbb{R}$, and $\phi(x):\mathbb{R}^n\rightarrow\mathbb{R}^{nxh}$ is a mapping to a high-dimensional feature space, and b is the bias term.

To construct the LSSVR model, it is essential to set parameters (C,γ), which are crucial for the successful establishment of the model. The regularization parameter (C) determines the penalty imposed on data points that deviate from the regression function, whereas the kernel parameter (γ) affects the smoothness of the regression function. In this study, we utilize an efficient optimization algorithm (JS) to obtain the optimal values of C and γ, ensuring the generation of the best LSSVR model.

2.2 Jellyfish search optimization algorithm

The jellyfish search optimizer (JS) was developed by Chou and Truong in 2021 [39]. This optimizer is inspired by the behavior of jellyfish in the ocean and consists of three main components: 1) ocean current, 2) Jellyfish Swarm, 3) time control system.

2.2.1 Ocean current

The direction of the ocean current $(\overrightarrow{trend})$ and the updated location are formulated as follows:

$$\overrightarrow{trend}=X^{*}-3\times\mathrm{rand}(0,1)\times\mu, \tag{2}$$

where X^{*} represents the jellyfish currently with the best location in the swarm, and μ denotes the mean location of all jellyfish.

2.2.2 Jellyfish swarm

A swarm consists of a large group of jellyfish that either move around one another's positions or remain in their own positions (passive motion, Type A). Type A refers to the movement of jellyfish around their own locations, with each jellyfish's most recent position being determined by.

$$X_i(t+1)=X_i(t)+0.1\times\mathrm{rand}(0,1)\times(Ub-Lb), \tag{3}$$

where Ub and Lb represent the upper and lower bounds of the search space, respectively.

Type B motion is simulated by Eqs. (6) and (7).

$$\overrightarrow{Step}=X_i(t+1)-X_i(t), \tag{4}$$

$$\overrightarrow{Step}=\mathrm{rand}(0,1)\times\overrightarrow{Direction}, \tag{5}$$

$$\overrightarrow{Direction}=\begin{cases}X_i(t)-X_j(t), & \text{if } f(X_j)\geqslant f(X_i),\\ X_j(t)-X_i(t), & \text{if } f(X_j)<f(X_i),\end{cases} \tag{6}$$

$$X_i(t+1)=X_i(t)+\overrightarrow{Step}. \tag{7}$$

2.2.3 Time control system

Equation (8) defines the time control function. If its value exceeds C_o, the jellyfish follow the ocean current; if its value is less than C_o, they move within the jellyfish bloom. C_o is set to 0.5, representing the mean between zero and one.

$$c(t)=\left|\left(1-\frac{t}{Max_{iter}}\right)\times(2\times\mathrm{rand}(0,1)-1)\right|, \tag{8}$$

where t represents the time specified as the number of iterations, and Max_{iter} is the maximum number of iterations, considered as an initialized parameter [39].

2.3 Jellyfish search-least square support vector regression

The suggested ML model was trained using the learning data shown in Fig. 1. The learning procedure for the proposed JS-LSSVR hybrid model unfolded as follows.

The JS algorithm generated a population of jellyfish in the search space. Specifically, 50 jellyfish were constructed with their respective coordinates. As outlined in Subsection 2.1, the coordinates of each jellyfish represent the radial basis function (RBF) width (γ) and regularization parameter (C) of the LSSVR model.

After this division, the learning data were split into training data (70%) and validation data (30%) based on a ratio proposed in earlier research [34]. Subsequently, the LSSVR models were trained using the training data, and the trained models were optimized using the validation data. The jellyfish coordinates were updated during each iteration of the optimization process, and the performance of the JS-LSSVR hybrid model was assessed and improved using the root-mean-square error (*RMSE*) as the objective function. Subsection 2.2 provides detailed information about the JS optimizer. The objective function of the proposed JS-LSSVR hybrid model is defined as follows.

$$f(C,\gamma)=RMSE^{\text{Traningprocess}}_{\text{ValidationData}}=\sqrt{\frac{1}{n_v}\sum_{i=1}^{n_v}(y_i'-y_i)^2}, \tag{9}$$

where y_i' and y_i are the predicted and actual values, respectively. Search space: $C_{min}\leqslant C\leqslant C_{max}$ and $\gamma_{min}\leqslant\gamma\leqslant\gamma_{max}$, n_v is the number of validation samples.

2.4 Evaluation of the prediction system

2.4.1 Cross-fold validation

A K-fold cross-validation procedure is commonly

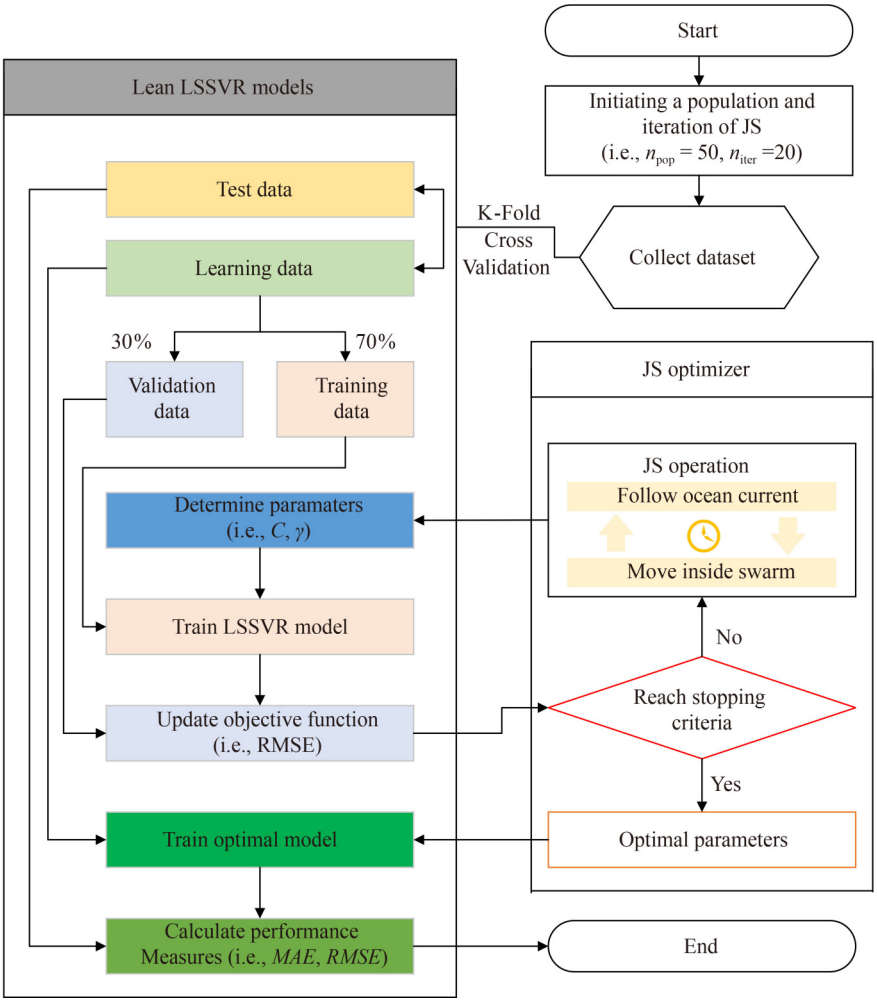

Fig. 1 Flowchart of the JS-LSSVR hybrid model.

employed to assess predictive performance, mitigating bias introduced by randomly selected training and test data. Cross-validation stratifies the folds by randomly distributing individual instances across various folds, ensuring that the proportions of predictor labels (responses) in the folds closely resemble those in the original data set. In this study, 10-fold cross-validation was utilized to evaluate the prediction consistency of the system. This number of folds was determined to be optimal based on prior research [41].

2.4.2 Performance metrics

In this study, three commonly used performance indicators were employed to assess the predictive capability of the proposed system, as suggested by Chou et al. [42] and Erdal et al. [43]. These indicators include the mean absolute error (*MAE*), the *RMSE*, and the *R*, as defined in Eqs. (10)–(12). The *MAE* represents the average of the absolute differences in values between the observed and predicted values generated by the ML models. *RMSE* measures the difference between values predicted by an ML model and the actual values. *R* values indicate the relationship between the actual and predicted values of the ML model [44].

$$R = \frac{n\sum y_i \cdot y_i' - (\sum y_i)(\sum y_i')}{\sqrt{n(y_i^2) - (\sum y_i)^2}\sqrt{n(\sum y_i'^2) - (\sum y_i')^2}}, \tag{10}$$

$$RMSE = \sqrt{\frac{1}{n}\sum_{i=1}^{n}(y_i - y_i')^2}, \tag{11}$$

$$MAE = \frac{1}{n}\sum_{i=1}^{n}\left|y_i - y_i'\right|, \tag{12}$$

where y' and y are the predicted and actual values, respectively; n is the number of samples.

3 Punching shear strength of flat slabs data

3.1 Data collection

Figure 2 illustrates an example of the punching shear

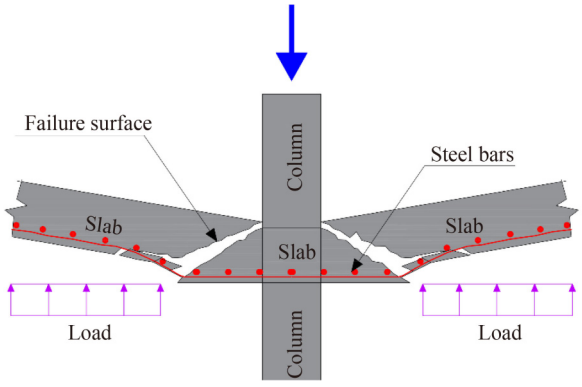

Fig. 2 Punching shear failure mode in flat slabs.

failure mode in RC flat slabs [34]. Experimental data comprising 511 valid samples were collected from literature published between 1938 and 2019 [9,10,19–21, 45–70]. The complete set of experimental data are provided in Table A1 in Electronic Supplementary materials. For the development of the ML models, 11 input variables were considered, including specimen length (X1), column size (X2), effective depth (X3), concrete compressive strength (X4), yield strength of steel re-bars (X5), reinforcement ratio at the top and bottom of the slab (X6, X7), specimen thickness (X8), elastic modulus of concrete (X9), and column type (X10, X11). Table 1 presents the statistical characteristics of the 11 input variables (X1–X11) and the output variable (Y) in the experimental data set comprising 511 samples.

3.2 Data preprocessing

Figure 3 displays the feature correlation matrix of the 11 input variables in the experimental data set comprising 511 samples. It is evident that X4 and X9 exhibit a strong correlation, leading to the removal of X9 from the model construction. To create a prediction model, the training data are normalized to the range [0,1]. This normalization is essential to prevent attributes with larger numerical ranges from overshadowing those with smaller ones and to avoid numerical difficulties, as described in Eq. (13) [71].

$$x_i^{\text{nor}} = \frac{x_i - x_{\min}}{x_{\max} - x_{\min}}, \tag{13}$$

where x_i is the input data point, $x_{\min}$ is the minimum value, $x_{\max}$ is the maximum value, and x_i^{nor} is the normalized value of the data.

3.3 Removing outliers

Extreme outliers outside the fences of the original data set were identified and removed using a box plot analysis. Figure 4 illustrates the box plot of the original data set, following which 22 extreme outliers exceeding the upper outer fence were eliminated. After this removal process, there were 489 samples remaining. These samples exhibited a minimum value of 0.0110 (MN), a maximum value of 1.3810, an average of 0.3728, and a standard deviation of 0.2604. Prediction models for the punching shear strength of RC flat slabs were subsequently developed using the generated samples that fell within the study's parameters.

4 Model evaluation

As mentioned in Subsection 2.3, optimizing the LSSVR hyperparameters, namely the regularization parameter (C) and the gamma parameter (γ) of the RBF kernel, is crucial for obtaining an accurate solution for predicting the punching shear strength of RC flat slabs. This constitutes a two-dimensional optimization problem. In

Table 1 Statistical characteristics of punching shear strength data set

Symbol	Attribute	Unit	Type	Min	Max	Std.
X1	specimen length	m	numeric	0.2000	5.7000	0.6657
X2	column size	m	numeric	0.0250	0.9010	0.1123
X3	effective depth	m	numeric	0.0350	0.5000	0.0592
X4	concrete compressive strength	MPa	numeric	8.5915	119.0000	19.2422
X5	yield strength of steel re-bars	MPa	numeric	255.000	811.0000	94.1199
X6	reinforcement ratio at the top of the slab	–	–	0.0022	0.2250	0.0148
X7	reinforcement ratio at the bottom of the slab	–	–	0.0000	0.0180	0.0036
X8	specimen thickness	m	numeric	0.0455	0.7620	0.0780
X9	elastic modulus of concrete	MPa	numeric	13776.3320	51270.9469	6827.3820
X10	square column type	–	categorical	0	1	–
X11	circle column type	–	categorical	0	1	–
Y	punching shear resistance	MN	numeric	0.0110	2.6810	0.4175

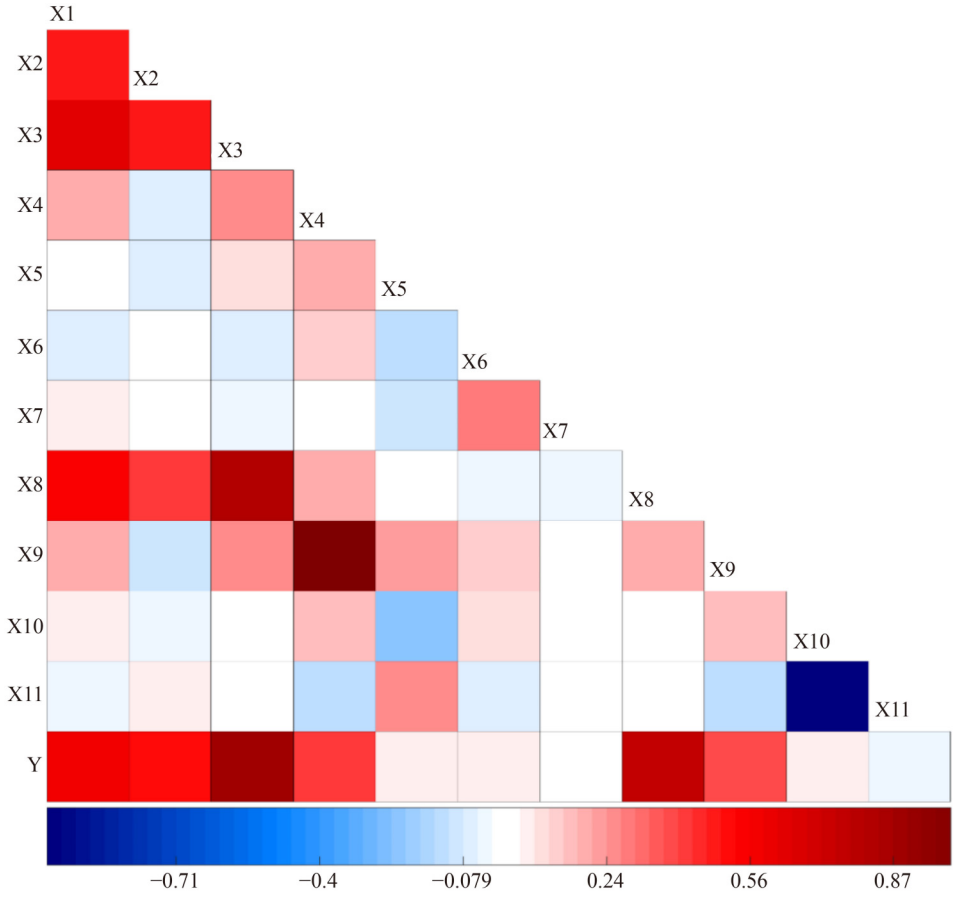

Fig. 3 Feature correlation matrix for punching shear strength data set.

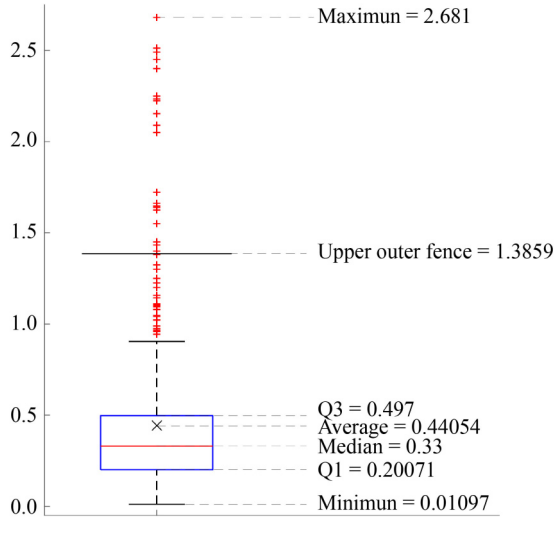

Fig. 4 Box plot of the original data set (unit: MN).

this study, the JS algorithm was employed as a search engine to enhance the values of C and γ. Specifically, $C$and γwere allowed to vary within broad ranges of $[0.001,10^{15}]$ and $[0.001,10^{9}]$, respectively. The population of JS consisted of 50 pairs of LSSVR hyperparameters (C and γ). The optimization process continued until the halting criteria were met, which were defined as reaching a maximum of 25 iterations or when consecutive rates of change in the objective function were less than 0.000001. At that point, the optimal hyperparameters for LSSVR were determined in Table 2.

Table 2 Optimal values for least squares SVR hyperparameters

Fold No.	Regularization parameter, C	Kernel parameter, γ
1	2.0230×10^{13}	116811.2957
2	3.4279×10^{13}	59433275.6036
3	1.9604×10^{13}	190384.6682
4	2.6947×10^{13}	215769.0747
5	703.6472	6.3849
6	5.1162×10^{13}	84469.8523
7	1.1625×10^{14}	39003.8533
8	3.3484×10^{13}	128558322.1544
9	3.5765×10^{13}	52169046.4106
10	1.7363×10^{13}	39534306.2050

The results indicate that, in the cross-validation approach, JS optimized the ranges of C and γ as $[703.6472,1.1625 \times 10^{14}]$ and [6.3849,128558322.1544], respectively, for predicting the punching shear strength of RC flat slabs. The performance metrics achieved by the

proposed JS-LSSRVR hybrid model during the learning and testing phases are summarized in Table 3. For the testing data set, the JS-LSSVR hybrid model exhibited average *RMSE*, *MAE*, and *R* values of 0.0067, 0.0503, and 0.9524, as shown in Table 3, indicating the model's effectiveness. Notably, the proposed system's best *RMSE* value during the cross-validation method was 0.0029 in fold 1, the best *MAE* value was 0.0400 in fold 5, and the best *R*-value was 0.9757 in fold 5.

Figure 5 illustrates the observed (actual) and predicted punching shear strengths of concrete flat slabs for 10-folds. The linear correlation (*R*) patterns demonstrate the model's strong prediction performance for the punching shear strength property of randomly distributed concrete flats.

Subsequently, the JS optimizer was compared with other well-known optimizers, including the ABC algorithm [72], DE algorithm [73], GA [74], GWO [75], PSO [76], TLBO [77], and WO [78], for searching hyperparameters in this problem. Once again, the optimal

Table 3 Optimal values for least squares SVR hyperparameters

Fold No.	Learning data			Test data		
	RMSE	*MAE*	*R*	*RMSE*	*MAE*	*R*
1	0.0012	0.0363	0.9815	0.0029	0.0554	0.9451
2	0.0055	0.0497	0.9599	0.0145	0.0419	0.9715
3	0.0130	0.0421	0.9768	0.0079	0.0442	0.9718
4	0.0035	0.0426	0.9733	0.0037	0.0479	0.9755
5	0.0000	0.0191	0.9942	0.0082	0.0400	0.9757
6	0.0135	0.0368	0.9841	0.0029	0.0417	0.9446
7	0.0184	0.0470	0.9763	0.0041	0.0684	0.9432
8	0.0234	0.0569	0.9547	0.0049	0.0629	0.9149
9	0.0097	0.0510	0.9627	0.0088	0.0555	0.9264
10	0.0017	0.0487	0.9629	0.0094	0.0447	0.9558
Min	0.0000	0.0191	0.9547	0.0029	0.0400	0.9149
Max	0.0234	0.0569	0.9942	0.0145	0.0684	0.9757
Average	0.0090	0.0430	0.9726	0.0067	0.0503	0.9524

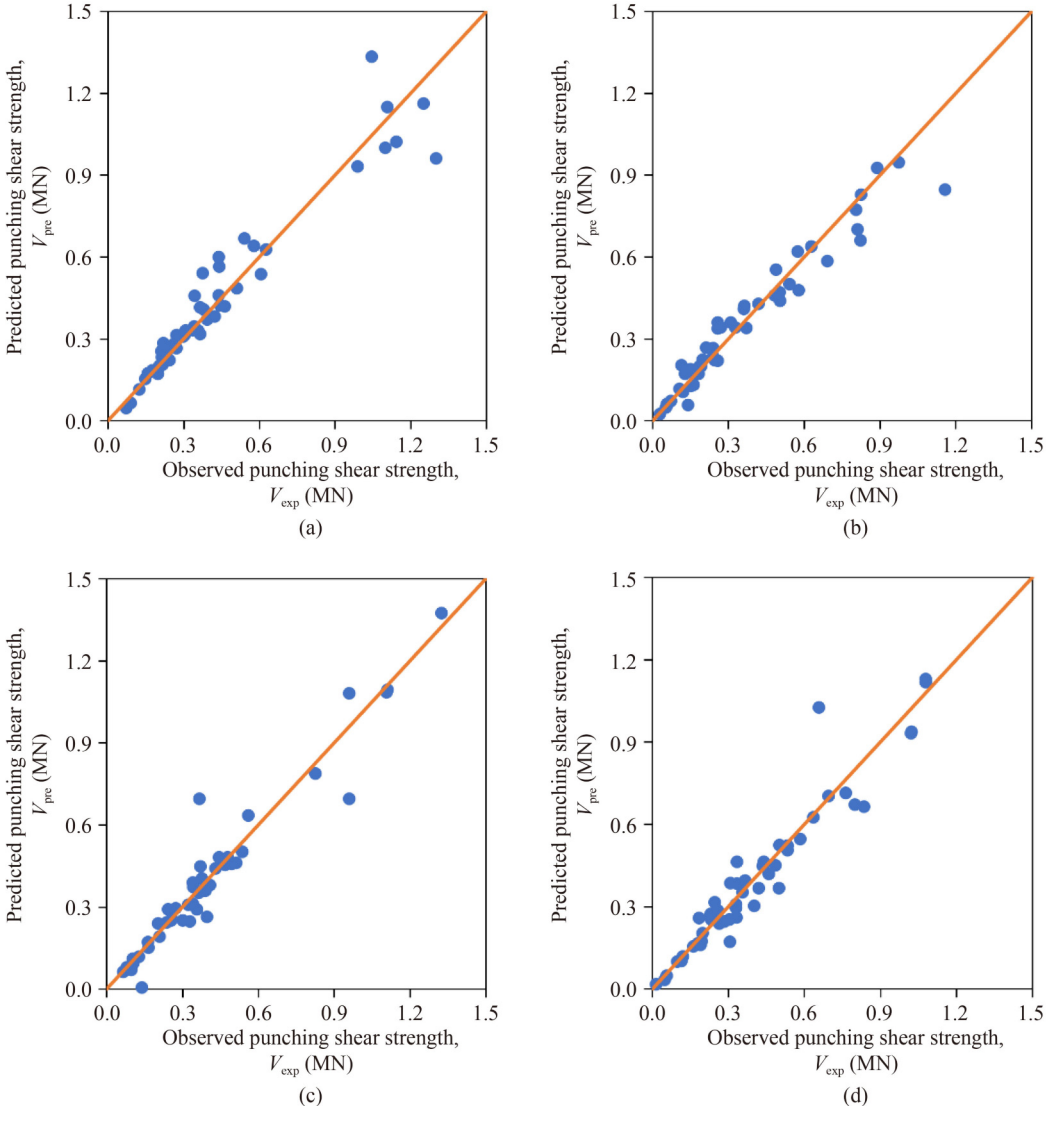

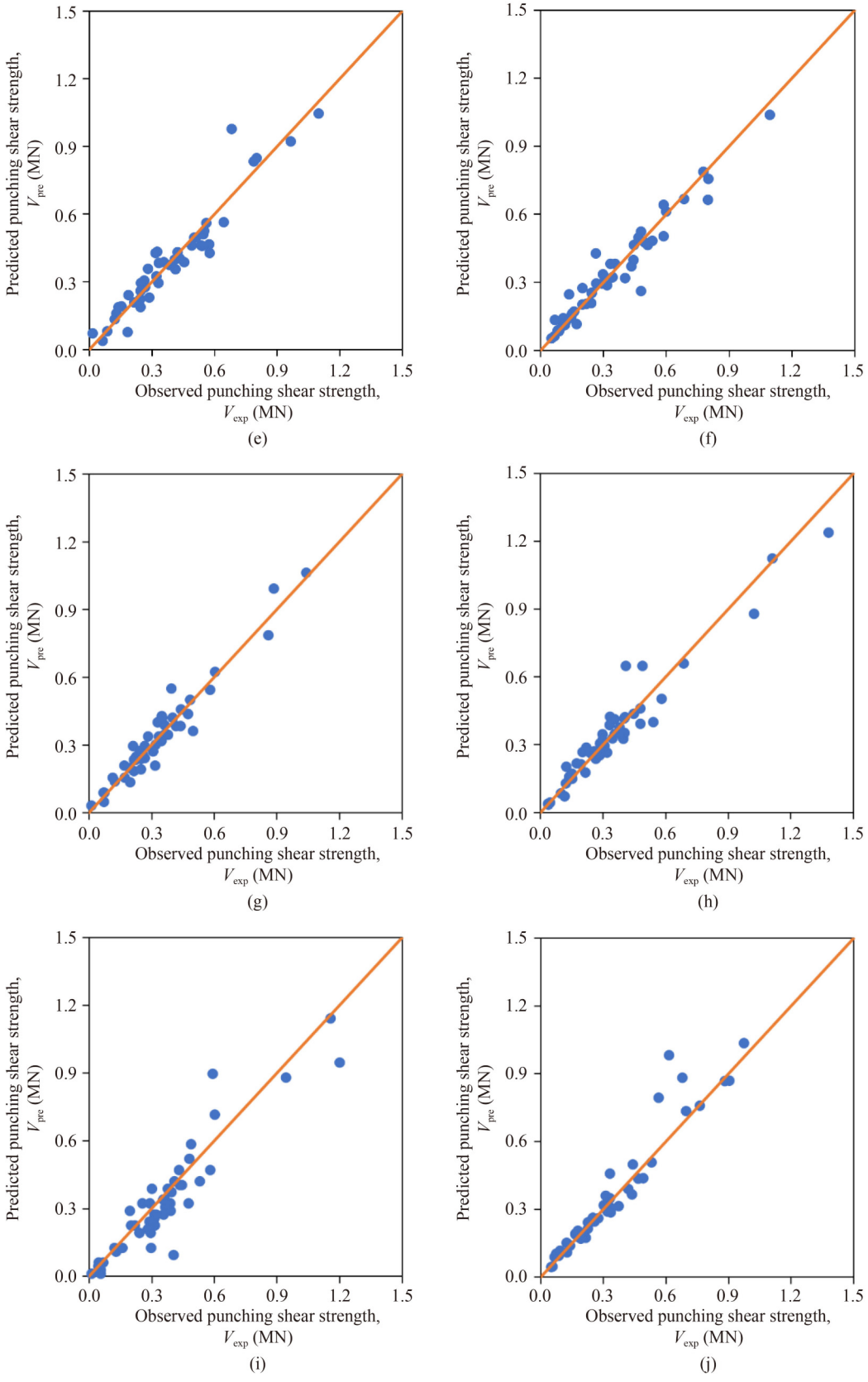

Fig. 5 Observed and predicted punching shear strength of concrete flat slabs in test data for 10-folds: (a) test data of fold 1; (b) test data of fold 2; (c) test data of fold 3; (d) test data of fold 4; (e) test data of fold 5; (f) test data of fold 6; (g) test data of fold 7; (h) test data of fold 8; (i) test data of fold 9; (j) test data of fold 10.

hyperparameters of the LSSVR were determined when the specified stopping criteria were met, set as a maximum of 25 iterations or consecutive rates of change in the objective function values less than 0.000001, as mentioned earlier. The individual parameters for the compared algorithms were kept at default settings in the program. The results presented in Table 4 indicate that both *RMSE* and *MAE* obtained by JS were lower than those obtained by the compared algorithms, and the *R* obtained by JS was higher. Moreover, the box plots of *RMSE*, *MAE*, and *R* from *K*-folds in Fig. 6 demonstrate that the mean and error achieved by the LSSVR algorithm using Jellyfish optimization were lower than those obtained by the compared optimizers. Additionally, the convergence graph of JS on the validation data consistently outperformed the compared algorithms across 10-folds, as shown in Fig. 7.

Furthermore, a comparison between the developed JS-

Table 4 Performance of JS vs. well-known optimizers in searching hyper paramters for the punching shear strength of RC flat slabs model

Model	*RMSE* (MN)	*MAE* (MN)	*R*
ABC-LSSVR	0.2876	0.7298	0.1518
DE-LSSVR	0.2747	0.6054	0.3727
GA-LSSVR	0.0144	0.0610	0.9353
GWO-LSSVR	0.1917	0.6752	0.3325
JS-LSSVR (this study)	0.0067	0.0503	0.9524
PSO-LSSVR	0.2889	0.6396	0.2904
TLBO-LSSVR	0.3004	0.7527	0.1309
WOA-LSSVR	0.2140	0.6449	0.3353

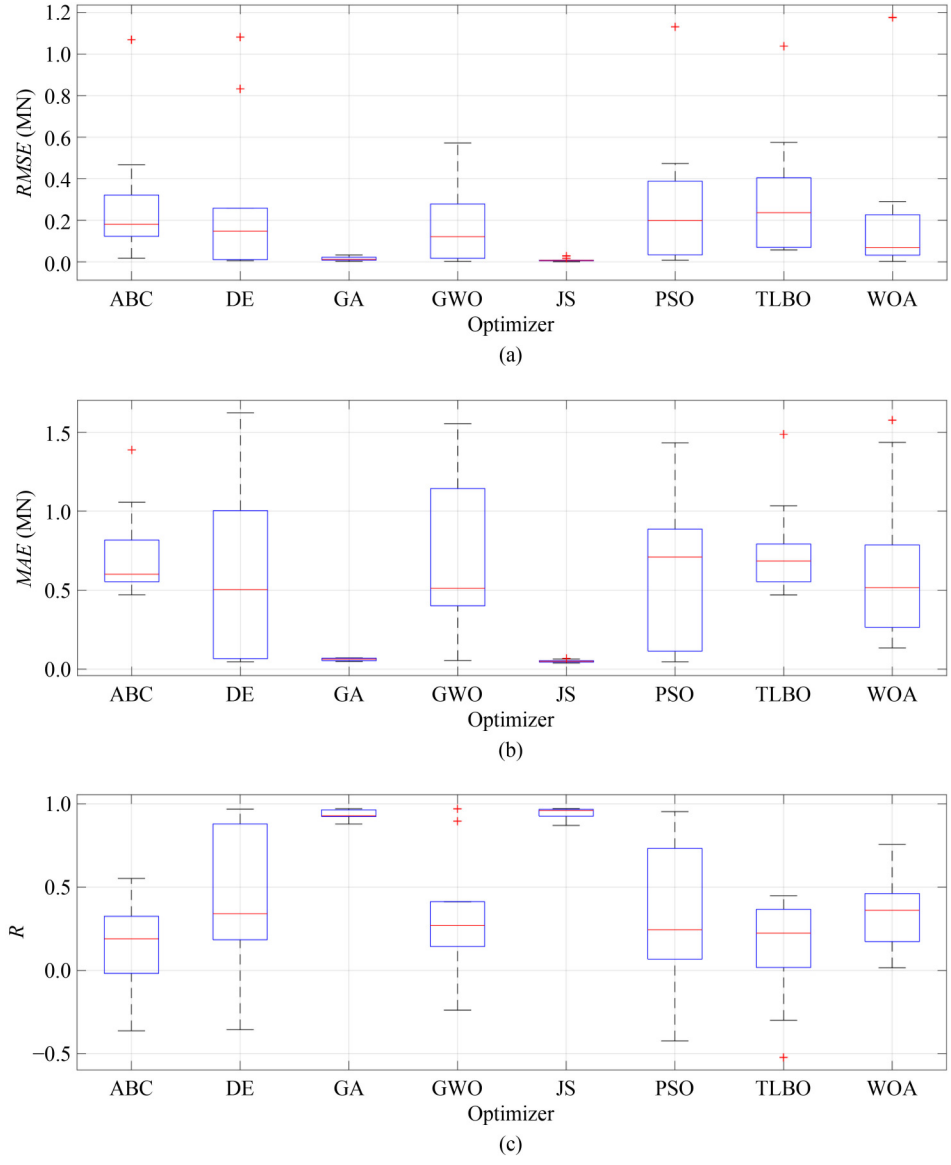

Fig. 6 Boxplot of *RMSE*, *MAE*, and *R* of LSSVR model using various optimizers: (a) boxplot of *RMSE*; (b) boxplot of *MAE*; (c) boxplot of *R*.

LSSVR model and five ML-based models from the literature (SVR [34], ANN [33], XGBoost [79], AdaBoost [34], PSO-SVR [35]), and other well-known ML methods (Gaussian process regression (GPR), Kernel-based regression (KBR), CatBoost, LightGBM, and Keras) was conducted and is presented in Table 5 and Fig. 8. Interestingly, the R for all the models are quite similar, but the performance estimator, *RMSE*, of the JS-LSSVR hybrid model is significantly smaller compared to these ML-based models. The differences were

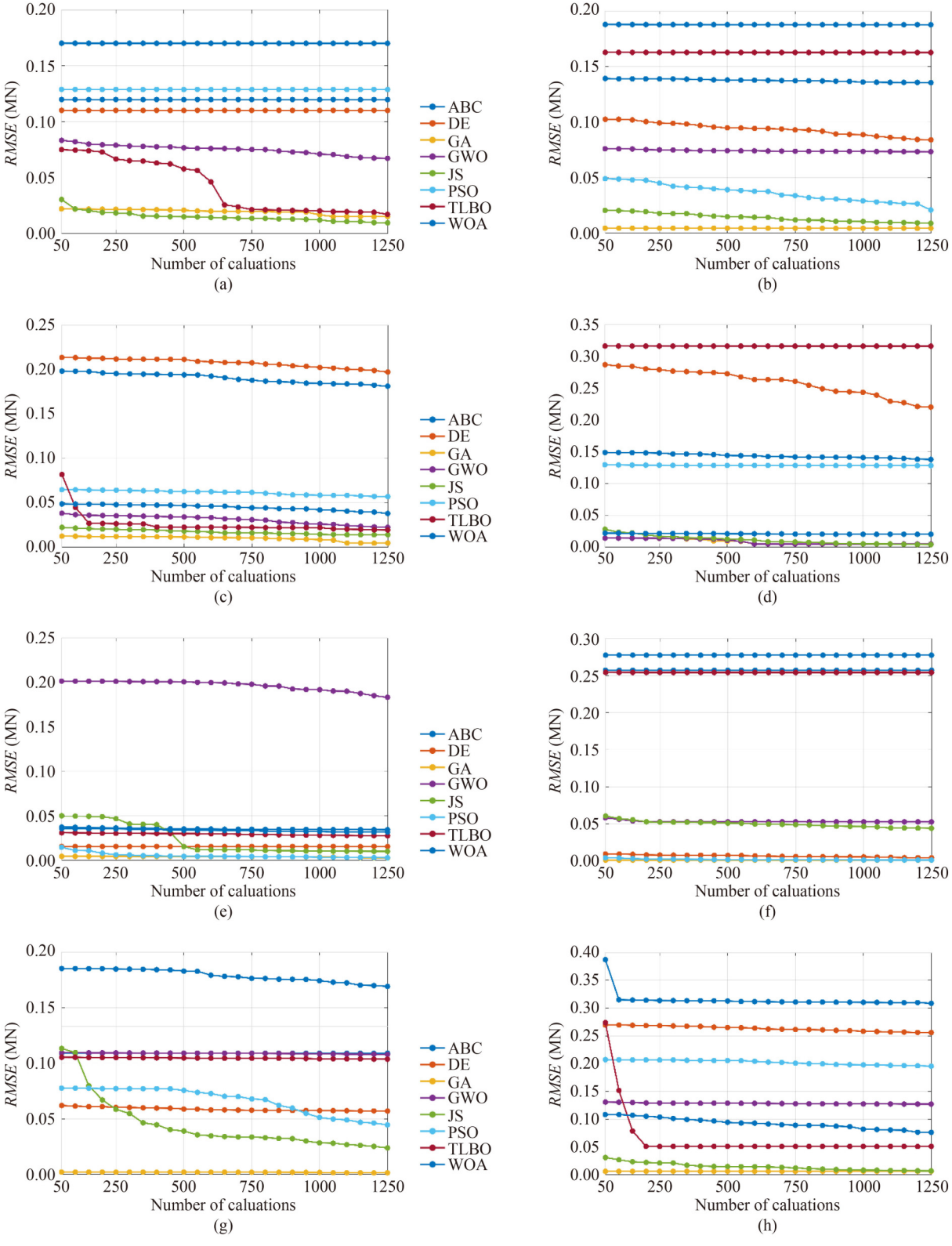

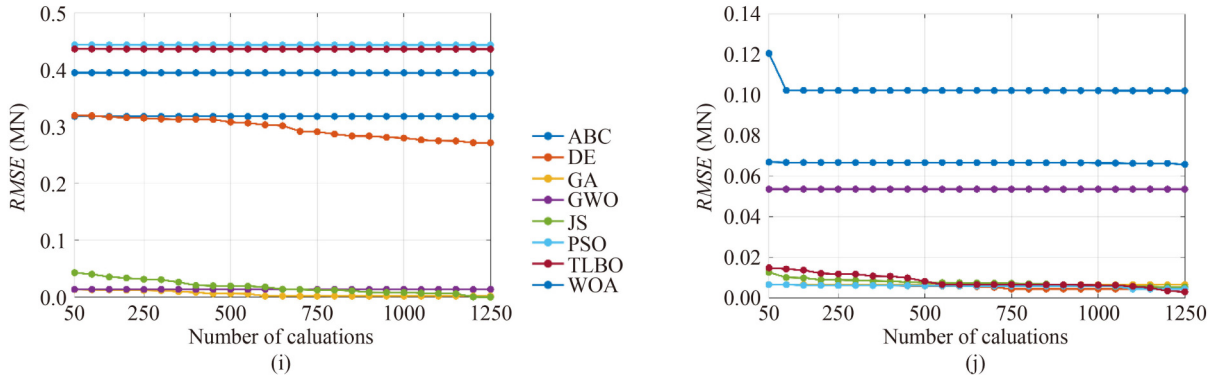

Fig. 7 Convergence comparisons on validation data: (a) convert graph of fold 1; (b) convert graph of fold 2; (c) convert graph of fold 3; (d) convert graph of fold 4; (e) convert graph of fold 5; (f) convert graph of fold 6; (g) convert graph of fold 7; (h) convert graph of fold 8; (i) convert graph of fold 9; (j) convert graph of fold 10.

approximately 89.80%, 85.75%, and 96.44% smaller for XGBoost [79], ANN [33], and PSO-SVR [35], respectively. This comparative analysis reveals that the JS-LSSVR model surpasses the previously studied ML models in terms of precision and accuracy.

One of the factors contributing to the enhanced prediction performance of the JS-LSSVR model is the utilization of a larger data set. This study employed a substantial number of experimental data points (511 specimens), surpassing the smaller data sets used in the ML models investigated by Nguyen et al. [79] (497 specimens), Tran and Kim [33] (218 specimens), and Wu and Zhou [35] (218 specimens). The increased quantity of data contributes to a more robust and comprehensive training of the JS-LSSVR model, leading to improved predictive capabilities.

Moreover, differences in the input variables used to train the ML models in the literature contribute to variations in prediction results. Previous studies employed six specific design parameters as input variables for their ML models, while the JS-LSSVR model might have incorporated a different set of input variables. These disparities in input variables could impact the reliability and accuracy of predictions, favoring the JS-LSSVR model due to the selection of more informative or relevant input features.

5 Comparison with current design codes

In Fig. 9, the relationship between the observed and predicted punching shear strength, as per various design codes (Table A2) including ACI 318-19 [19], KDS 14 20 22 [3], Eurocode 2 [20], BS 8110 [21], and JS-LSSVR (for data in fold 5), is presented. Upon comparing the

Table 5 Prediction performance of various models for the punching shear strength of RC flat slabs

No.	Model	*RMSE* (MN)	*MAE* (MN)	*R*
1	JS-LSSVR (this study)	0.0067	0.0503	0.9524
2	GPR (this study)	0.0076	0.0492	0.9550
3	KBR (this study)	0.0064	0.0509	0.9443
4	CatBoost (this study)	0.1128	0.0611	0.9604
5	LightGBM (this study)	0.0921	0.0565	0.9326
6	Keras (this study)	0.1162	0.0662	0.9353
7	SVR [34]	–	–	0.8349
8	ANN [33]	0.0470	–	0.9965
9	XGBoost [79]	0.0657	–	0.9787
10	AdaBoost [34]	–	–	0.8758
11	PSO-SVR [35]	0.1880	0.135889	0.9706

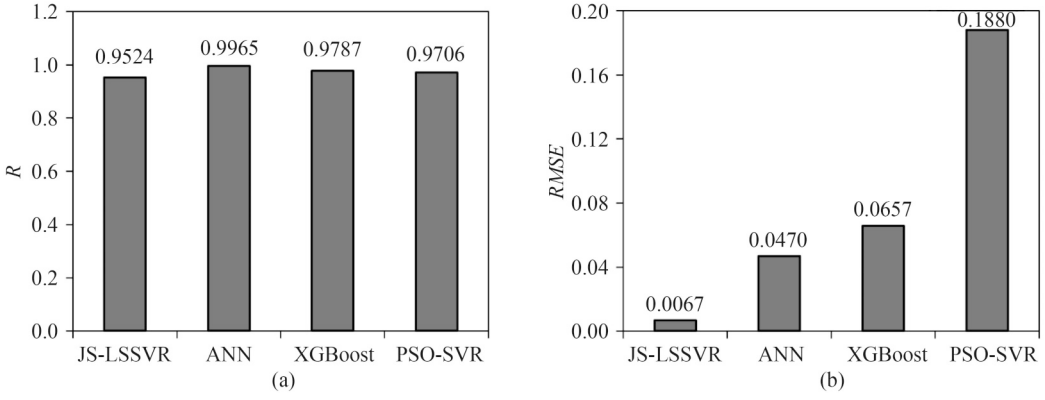

Fig. 8 Comparison of prediction performance of JS-LSSVR and existing ML-based models: (a) *R*; (b) *RMSE*.

prediction results of the JS-LSSVR model in Fig. 9(e) with the other design codes, it is evident that most current design codes exhibit a higher scatter, indicating less accurate predictions.

Among the four design codes depicted in Fig. 9(d), BS 8110 [21] demonstrates the best performance with an *R*-value of 0.9625 and an *RMSE* value of 0.0725. Eurocode 2 [20] closely follows with an *R*-value of 0.9471 and an *RMSE* value of 0.0857, as shown in Fig. 9(c). KDS 14 20 22 exhibits an *R*-value of 0.8856 and an *RMSE* value of 0.1241 in Fig. 9(b), while ACI 318-19 shows an *R*-value of 0.8716 and an *RMSE* value of 0.1309 in Fig. 9(a). It is important to note that these results are significantly poorer compared to those of the JS-LSSVR model.

Moreover, the ACI 318-19, Eurocode 2, and BS 8110 design codes tend to provide conservative predictions for

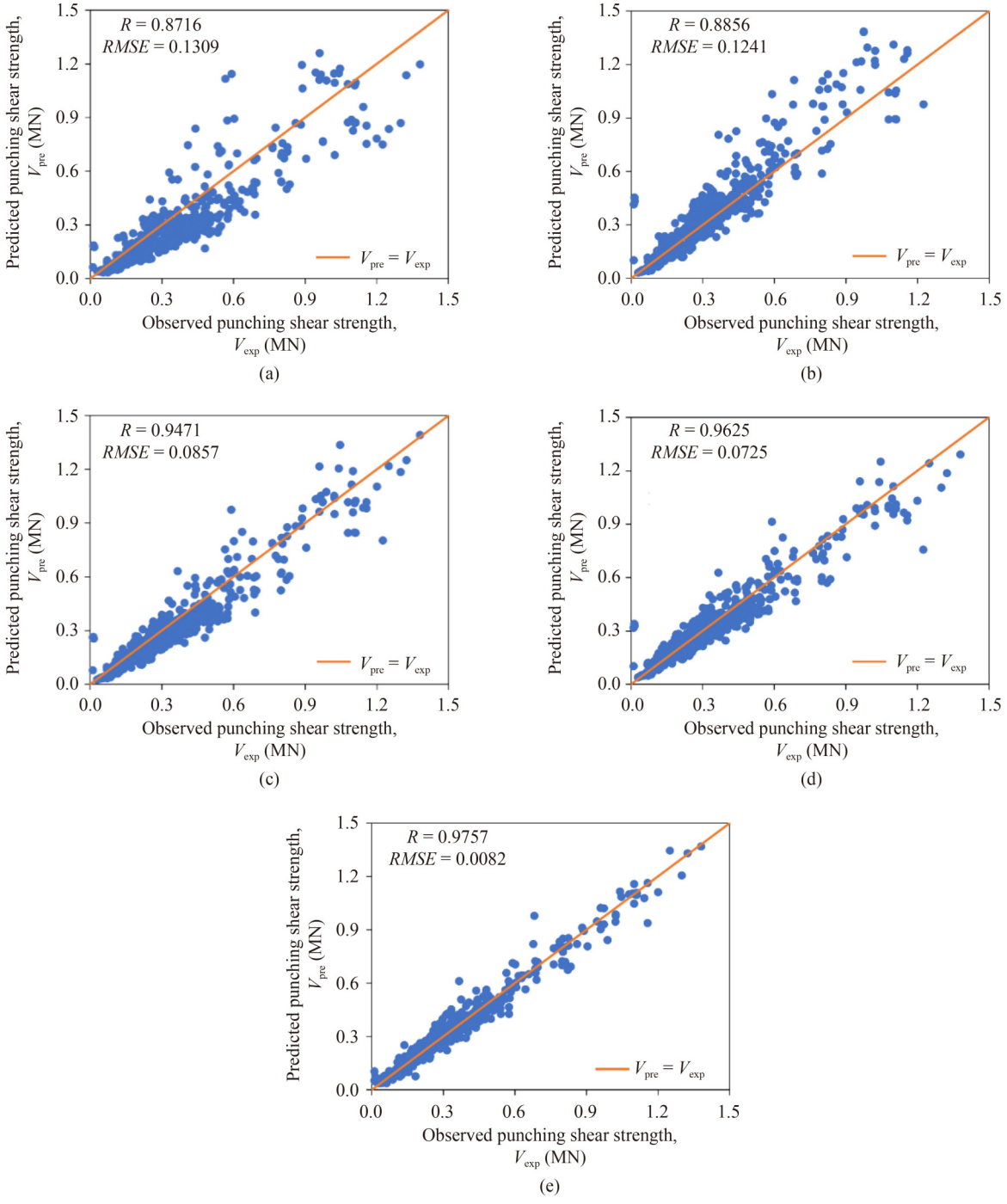

Fig. 9 Scatter plots comparing current design codes and the JS-LSSVR model for predicting the punching shear strength of RC flat slabs: (a) ACI 318-19; (b) KDS 14 20 22; (c) Eurocode 2; (d) BS 8110; (e) JS-LSSVR.

approximately 81%, 75%, and 60% of the samples, respectively, indicating a lower-bound design approach. Conversely, KDS 14 20 22 tends to overestimate the punching shear capacities of RC flat slabs in approximately 60% of the cases. This overestimation could be attributed to limitations in the longitudinal reinforcement ratio and the modification of size-effective factors in KDS 14 20 22.

Figure 10 illustrates a comparison of the observed-to-predicted ratio of punching shear strength as a function of the effective depth of RC flat slabs, considering the current design codes and the JS-LSSVR model (for data in fold 5). Among the four design codes, BS 8110 (Fig. 10(d)) demonstrates a mean value and coefficient of variation (*COV*) of 1.048 and 0.179, respectively, indicating higher accuracy compared to Eurocode 2 (mean = 1.187, *COV* = 0.216, Fig. 10(c)), KDS 14 20 22 (mean = 0.987, *COV* = 0.238, Fig. 10(b)), and ACI 318-19 (mean = 1.336, *COV* = 0.268, Fig. 10(a)). The differences in mean and *COV* between BS 8110 and Eurocode 2, KDS 14 20 22, and ACI 318-19 are 13.3% and 20.7%, 5.8% and 33.0%, and 27.5% and 49.7%,

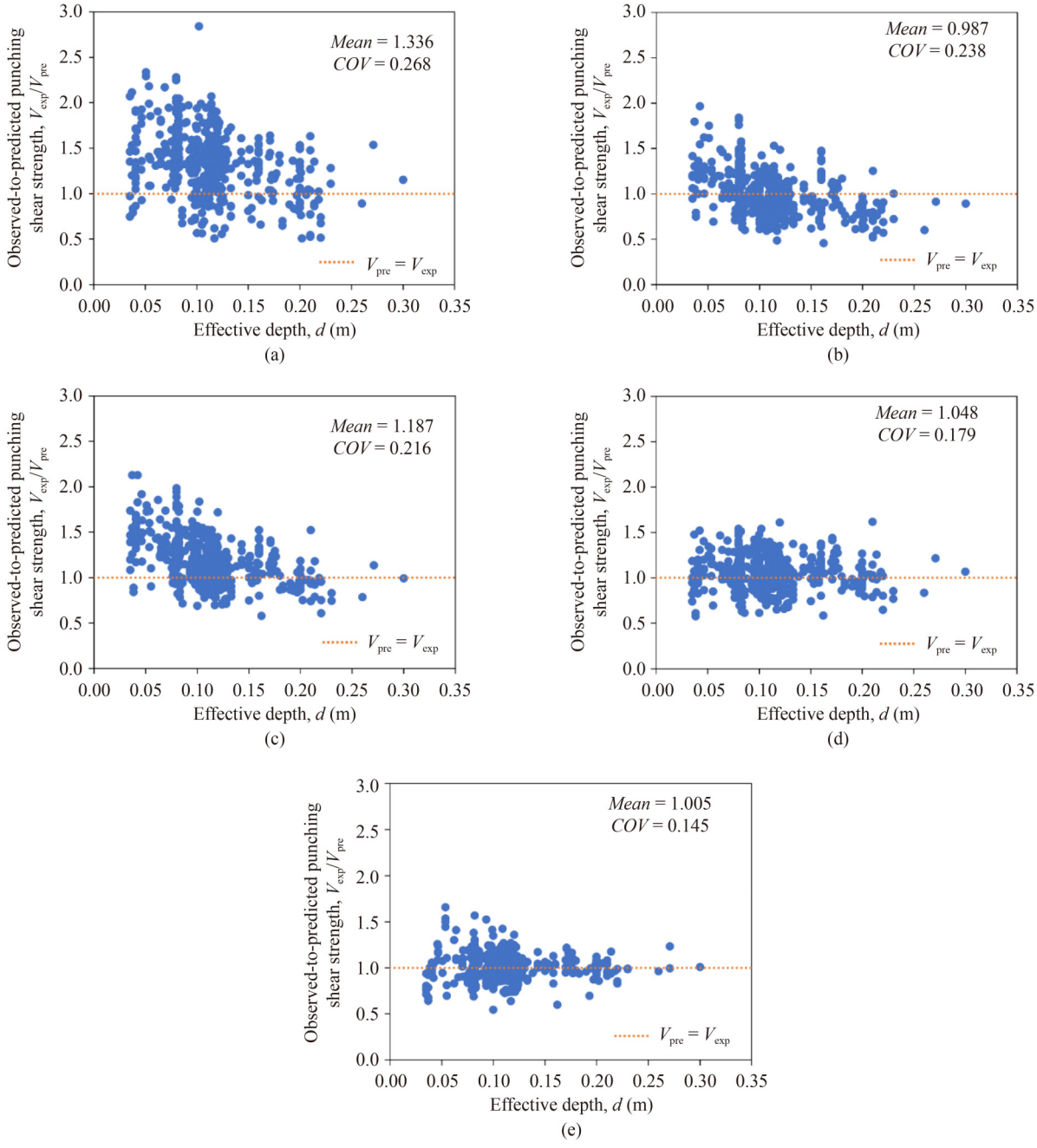

Fig. 10 Variation of current design codes and JS-LSSVR model according to effective depth: (a) ACI 318-19; (b) KDS 14 20 22; (c) Eurocode 2; (d) BS 8110; (e) JS-LSSVR.

respectively. Additionally, BS 8110 shows less biased observed-to-predicted ratios compared to the other design codes.

In Fig. 10(e), the JS-LSSVR model shows an observed-to-predicted ratio mean of 1.005, with a *COV* of 0.145. This comparison reveals that the JS-LSSVR model provides more accurate and unbiased predictions than the current design codes. When compared to the best mechanics-based model, BS 8110, the JS-LSSVR model achieves a significant reduction of 4.1% and 19.0% in the mean value and *COV*, respectively, demonstrating superior performance in estimating punching shear strength. Particularly for RC flat slabs with a larger effective depth ($d \geqslant 0.15$ m), the JS-LSSVR model exhibits high accuracy and less biased observed-to-predicted ratios, unlike the current design codes, which appear to be highly sensitive to the slab's depth.

In Fig. 11, the distribution of observed-to-predicted punching shear strength ratios (V_{exp}/V_{pre}), generated by the four current design codes and the JS-LSSVR model (for the data in fold 5), is presented. The results clearly demonstrate the significantly superior performance of the JS-LSSVR model compared to the current design codes. Specifically, when the JS-LSSVR model predicts punching shear strength ratios, there is a high concentration around 1.0. This indicates that the model provides predictions close to the observed values, resulting in a narrow distribution of the ratios. In contrast, for the design codes BS 8110, Eurocode 2, KDS 14 20 22, and ACI 318-19, the distribution of the V_{exp}/V_{pre} ratios becomes considerably wider. This wider distribution suggests that the predictions generated by these design codes deviate more from the observed values, leading to a less accurate and more scattered distribution of the ratios.

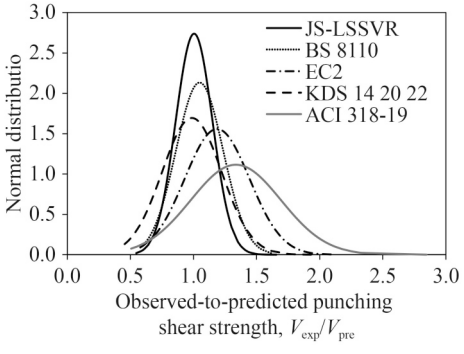

Fig. 11 Normal distribution of observed-to-predicted punching shear strength of current design codes and JS-LSSVR model.

Overall, the JS-LSSVR model outperforms the current design codes in terms of accuracy and prediction performance, as evidenced by the lower scatter and more favorable mean, *COV*, *R*, and *RMSE* values. This fact indicates that while the design codes are still widely used, there is room for improvement by considering combined approaches that integrate mechanics-based models and ML-based models to achieve highly accurate and less biased predictions in specific cases.

6 Conclusions

This study collected 511 samples from previous research to develop the JS-LSSVR hybrid model for predicting the punching shear strength of RC flat slabs. The original data set consisted of 511 samples and 11 features. However, 22 samples with one feature (X9) were removed to prevent distortion and maintain the integrity of the data set for building the JS-LSSVR hybrid model.

The JS-LSSVR hybrid model was created by combining the LSSVR algorithm with an advanced swarm intelligence optimization algorithm (JS). This integration enables the JS algorithm to effectively optimize the hyperparameters of the LSSVR algorithm, assisting civil engineers in designing the optimal punching shear strength of RC flat slabs.

To assess the generalization capability of the proposed hybrid model, a 10-fold cross-validation approach was employed. The results demonstrated that the proposed model has lower *RMSE* and *MAE* values than ABC-LSSVR, DE-LSSVR, GA-LSSVR, GWO-LSSVR, PSO-LSSVR, TLBO-LSSVR, and WOA-LSSVR models, as well as higher *R* values than those of the compared models. Additionally, the JS-LSSVR model achieved the lowest error (*RMSE*) when compared to existing ML-based models, namely ANN, XGBoost, and PSO-SVR.

The utilization of the proposed JS-LSSVR model led to a significant improvement in prediction performance when compared to current design codes such as ACI 318-19, KDS 14 20 22, Eurocode 2, and BS 8110. The enhanced performance of the JS-LSSVR model indicates its superiority in accurately predicting punching shear strength, surpassing the capabilities of existing design codes. This underscores the potential of the JS-LSSVR model to provide more reliable and precise predictions, offering a valuable alternative to conventional practices in the field of structural engineering.

Furthermore, this study employed a method to reduce feature dimensionality based on the distance *R*. However, the Pearson *R* has limitations; it requires variables to be normally distributed and can only identify linear correlations between them. When the Pearson *R* is 0, it cannot determine whether two variables are independent, suggesting that they might have a nonlinear relationship. Therefore, in future research, the distance correlation will be utilized to reduce the dimensionality of the feature parameters. Additionally, mutual information-based filter methods have gained popularity due to their ability to capture nonlinear correlations between dependent and independent variables in a machine-learning context. These methods will be considered in our upcoming research.

Acknowledgements This research was supported by the Research Program funded by Seoul National University of Science and Technology (SeoulTech). The authors are grateful for the support by the Research Program funded by Seoul National University of Science and Technology (SeoulTech).

Open Access This article is licensed under a Creative Commons Attribution 4.0 International License (https://creativecommons.org/licenses/by/4.0/), which permits use, sharing, adaptation, distribution and reproduction in any medium or format, as long as you give appropriate credit to the original author(s) and the source, provide a link to the Creative Commons licence, and indicate if changes were made. The images or other third party material in this article are included in the article's Creative Commons licence, unless indicated otherwise in a credit line to the material. If material is not included in the article's Creative Commons licence and your intended use is not permitted by statutory regulation or exceeds the permitted use, you will need to obtain permission directly from the copyright holder. To view a copy of this licence, visit http://creativecommons.org/licenses/by/4.0/.

Competing interests The authors declare that they have no competing interests.

References

1. Mellios N, Uz O, Spyridis P. Data-based modeling of the punching shear capacity of concrete structures. Engineering Structures, 2023, 275: 115195
2. Koppitz R, Kenel A, Keller T. Punching shear of RC flat slabs—Review of analytical models for new and strengthening of existing slabs. Engineering Structures, 2013, 52: 123−130
3. Truong G T, Choi K K, Kim C S. Punching shear strength of interior concrete slab-column connections reinforced with FRP flexural and shear reinforcement. Journal of Building Engineering, 2022, 46: 103692
4. Truong G T, Choi K K, Kim C S. Implementation of boosting algorithms for prediction of punching shear strength of RC column footings. Structures, 2022, 46: 521−538
5. Marques M G, Liberati E A P, Gomes R B, Carvalho A L, Trautwein L M. Punching shear strength model for reinforced concrete flat slabs with openings. Journal of Structural Engineering, 2021, 147(7): 04021090
6. Deng P, Matsumoto T. Fracture mechanics-based fatigue life prediction method for RC slabs in punching shear failure mode. Journal of Structural Engineering, 2020, 146(1): 04019186
7. Theodorakopoulos D D, Swamy R N. Ultimate punching shear strength analysis of slab-column connections. Cement and Concrete Composites, 2002, 24(6): 509−521
8. Metwally I M, Issa M S, El-Betar S A. Punching shear resistance of normal and high strength reinforced concrete flat slabs. Civil Engineering Research Magazine, 2008, 30(3): 982−1003
9. Birkle G, Dilger W H. Influence of slab thickness on punching shear strength. ACI Structural Journal, 2008, 105(2): 180
10. Rizk E, Marzouk H, Hussein A. Punching shear of thick plates with and without shear reinforcement. ACI Structural Journal, 2011, 108(5): 581
11. Shatarat N, Salman D. Investigation of punching shear behavior of flat slabs with different types and arrangements of shear reinforcement. Case Studies in Construction Materials, 2022, 16: e01028
12. Hoang L C, Pop A. Punching shear capacity of reinforced concrete slabs with headed shear studs. Magazine of Concrete Research, 2016, 68(3): 118−126
13. Alexander S B, Simmonds S H. Ultimate strength of slab-column connections. ACI Structural Journal, 1987, 84(3): 255−261
14. Huang C, Pu S, Ding B. An analytical punching shear model of RC slab-column connection based on database. Journal of Intelligent & Fuzzy Systems, 2018, 35(1): 469−483
15. Elshafey A A, Rizk E, Marzouk H, Haddara M R. Prediction of punching shear strength of two-way slabs. Engineering Structures, 2011, 33(5): 1742−1753
16. Deifalla A. A mechanical model for concrete slabs subjected to combined punching shear and in-plane tensile forces. Engineering Structures, 2021, 231: 111787
17. Kueres D, Siburg C, Herbrand M, Classen M, Hegger J. Uniform design method for punching shear in flat slabs and column bases. Engineering Structures, 2017, 136: 149−164
18. Park H G, Choi K K, Chung L. Strain-based strength model for direct punching shear of interior slab-column connections. Engineering Structures, 2011, 33(3): 1062−1073
19. ACI 318-19. Building Code Requirement for Structure Concrete. Farmington Hills, MI: American Concrete Institute, 2019
20. EN 1992-1-1. Eurocode 2: Design of Concrete Structures—Part I: General Rules and Rules for Buildings. Brussels: European Committee for Standardization, 2004
21. BS 8110. Structural Use of Concrete—Part I: Code of Practice for Design and Construction. London: British Standards Institution, 1997
22. Lou Y, Wu L, Liu L, Yu K, Liu N, Wang Z, Wang W. Irregularly sampled seismic data interpolation via wavelet-based convolutional block attention deep learning. Artificial Intelligence in Geosciences, 2022, 3: 192−202
23. Vu-Bac N, Silani M, Lahmer T, Zhuang X, Rabczuk T. A unified framework for stochastic predictions of mechanical properties of polymeric nanocomposites. Computational Materials Science, 2015, 96: 520−535
24. Vu-Bac N, Lahmer T, Zhuang X, Nguyen-Thoi T, Rabczuk T. A software framework for probabilistic sensitivity analysis for computationally expensive models. Advances in Engineering Software, 2016, 100: 19−31
25. Vu-Bac N, Areias P M A, Rabczuk T. A multiscale multisurface constitutive model for the thermo-plastic behavior of polyethylene. Polymer, 2016, 105: 327−338
26. Guo H, Zhuang X, Chen P, Alajlan N, Rabczuk T. Stochastic deep collocation method based on neural architecture search and transfer learning for heterogeneous porous media. Engineering with Computers, 2022, 38(6): 5173−5198
27. Guo H, Zhuang X, Chen P, Alajlan N, Rabczuk T. Analysis of three-dimensional potential problems in non-homogeneous media with physics-informed deep collocation method using material transfer learning and sensitivity analysis. Engineering with

Computers, 2022, 38(6): 5423−5444
28. Guo H, Zhuang X, Fu X, Zhu Y, Rabczuk T. Physics-informed deep learning for three-dimensional transient heat transfer analysis of functionally graded materials. Computational Mechanics, 2023, 72(3): 513−524
29. Choi K, Taha M M R, Sherif A G. Simplified punching shear design method for slab-column connections using fuzzy learning. ACI Structural Journal, 2007, 104(4): 438
30. Erdem H. Prediction of the moment capacity of reinforced concrete slabs in fire using artificial neural networks. Advances in Engineering Software, 2010, 41(2): 270−276
31. Akbarpour H, Akbarpour M. Prediction of punching shear strength of two-way slabs using artificial neural network and adaptive neuro-fuzzy inference system. Neural Computing & Applications, 2017, 28(11): 3273−3284
32. Chetchotisak P, Ruengpim P, Chetchotsak D, Yindeesuk S. Punching shear strengths of RC slab-column connections: Prediction and reliability. KSCE Journal of Civil Engineering, 2018, 22(8): 3066−3076
33. Tran V L, Kim S E. A practical ANN model for predicting the PSS of two-way reinforced concrete slabs. Engineering with Computers, 2021, 37(3): 2303−2327
34. Mangalathu S, Shin H, Choi E, Jeon J S. Explainable machine learning models for punching shear strength estimation of flat slabs without transverse reinforcement. Journal of Building Engineering, 2021, 39: 102300
35. Wu Y, Zhou Y. Prediction and feature analysis of punching shear strength of two-way reinforced concrete slabs using optimized machine learning algorithm and Shapley additive explanations. Mechanics of Advanced Materials and Structures, 2023, 30(15): 3086−3096
36. Vu-Bac N, Duong T X, Lahmer T, Zhuang X, Sauer R A, Park H S, Rabczuk T. A NURBS-based inverse analysis for reconstruction of nonlinear deformations of thin shell structures. Computer Methods in Applied Mechanics and Engineering, 2018, 331: 427−455
37. Vu-Bac N, Duong T X, Lahmer T, Areias P, Sauer R A, Park H S, Rabczuk T. A NURBS-based inverse analysis of thermal expansion induced morphing of thin shells. Computer Methods in Applied Mechanics and Engineering, 2019, 350: 480−510
38. Vu-Bac N, Rabczuk T, Park H S, Fu X, Zhuang X. A NURBS-based inverse analysis of swelling induced morphing of thin stimuli-responsive polymer gels. Computer Methods in Applied Mechanics and Engineering, 2022, 397: 115049
39. Chou J S, Truong D N. A novel metaheuristic optimizer inspired by behavior of jellyfish in ocean. Applied Mathematics and Computation, 2021, 389: 125535
40. Suykens J A K, van Gestel T, de Brabanter J, de Moor B, Vandewalle J. Least Squares Support Vector Machines. Singapore: World Scientific Publishing Company, 2002
41. Kohavi R. A study of cross-validation and bootstrap for accuracy estimation and model selection. In: Proceedings of the 14th International Joint Conference on Artificial Intelligence. San Francisco, CA: Morgan Kaufmann Publishers Inc., 1995
42. Chou J S, Hsu S C, Ngo N T, Lin C W, Tsui C C. Hybrid machine learning system to forecast electricity consumption of smart grid-based air conditioners. IEEE Systems Journal, 2019, 13(3): 3120−3128
43. Erdal H I, Karakurt O, Namli E. High performance concrete compressive strength forecasting using ensemble models based on discrete wavelet transform. Engineering Applications of Artificial Intelligence, 2013, 26(4): 1246−1254
44. Chou J S, Yang K H, Pampang J P, Pham A D. Evolutionary metaheuristic intelligence to simulate tensile loads in reinforcement for geosynthetic-reinforced soil structures. Computers and Geotechnics, 2015, 66: 1−15
45. Elstner R C, Hognestad E. Shearing strength of reinforced concrete slabs. ACI Journal Proceedings, 1956, 53(7): 29−58
46. Bažant Z P, Cao Z. Size effect in punching shear failure of slabs. ACI Structural Journal, 1987, 84(1): 44−53
47. Guandalini S, Burdet O, Muttoni A. Punching tests of slabs with low reinforcement ratios. ACI Structural Journal, 2009, 106: 87−95
48. Pralong J. Poinçonnement symétrique des planchers-dalles. Dissertation for the Doctoral Degree. Zurich: ETH Zurich, 1982 (in French)
49. Schaefers U. Design and safety against punching of rebar-free reinforced concrete ceilings in the area of the inner supports. Berlin: Ernst, 1984, 1–83 (in German)
50. Ladner M. Influence of the mabstabrobe in punching attempts—Derivation of a well-founded transfer law. Material and technology, 1973 (in German)
51. Kinnunen S, Nylander H. Punching of concrete slabs without shear reinforcement. Transport of the Royal Institute of Technology, 1960: 122
52. Tomaszewicz A. High Strength Concrete: SP2—Plates and Shells Report 2.3. Punching Shear Capacity of Reinforced Concrete Slabs. NOAA Technical Report 199409. 1993
53. Marzouk H, Hussein A. Experimental investigation on the behavior of high-strength concrete slabs. ACI Structural Journal, 1992, 88(6): 701−713
54. Regan P E. Symmetric punching of reinforced concrete slabs. Magazine of Concrete Research, 1986, 38(136): 115−128
55. Swamy R N, Ali S A R. Punching shear behavior of reinforced slab-column connections made with steel fiber concrete. ACI Journal Proceedings, 1982, 79(5): 392−406
56. Corley W G, Hawkins N M. Shearhead reinforcement for slabs. ACI Journal Proceedings, 1968, 65(10): 811−824
57. Fib Bulletin. Punching of Structural Concrete Slabs. Fib Bulletin Technical Report No. 12. 2001
58. Manterola M. Stamping ceramic tiles without sharpness. Dissertation for the Doctoral Degree. Lausanne: Federal Institute of Technology in Lausanne, 2011 (in French)
59. Niazi M S, Wisselink H H, Meinders T. Viscoplastic regularization of local damage models: Revisited. Computational Mechanics, 2013, 51(2): 203−216
60. Teng S, Cheong H K, Kuang K L, Geng J Z. Punching shear strength of slabs with openings and supported on rectangular columns. ACI Structural Journal, 2004, 101(5): 678−687
61. Li K. Influence of size on punching shear strength of concrete slabs. Thesis for the Master's Degree. Montreal: McGill University, 2000
62. Stein T, Ghali A, Dilger W. Distinction between punching and

flexural failure modes of flat plates. ACI Structural Journal, 2007, 104(3): 357

63. Papanikolaou K V, Tegos I A, Kappos A J. Punching shear testing of reinforced concrete slabs, and design implications. Magazine of Concrete Research, 2005, 57(3): 167−177
64. Ozden S, Ersoy U, Ozturan T. Punching shear tests of normal- and high-strength concrete flat plates. Canadian Journal of Civil Engineering, 2006, 33(11): 1389−1400
65. Bompa D V, Oneţ T. Punching shear strength of RC flat slabs at interior connections to columns. Magazine of Concrete Research, 2016, 68(1): 24−42
66. Hallgren M. Punching shear capacity of reinforced high-strength concrete slabs. Dissertation for the Doctoral Degree. Stockholm: Royal Institute Of Technology, 1998
67. Ramdane K. Punching shear of high performance concrete slabs. In: Proceedings of 4th International Symposium on Utilization of High-strength/High-performance Concrete. Paris: Pr. Ponts et Chaussées, 1996
68. Lovrovich J S, McLean D I. Punching shear behavior of slabs with varying span-depth ratios. ACI Structural Journal, 1990, 87(5): 507−512
69. Kinnunen S, Nylander H, Tolf P. Investigations on punching at the division of building statics and structural engineering. Nordisk Betong, 1978, 3: 25−27
70. Dönmez A, Bažant Z P. Size effect on punching strength of reinforced concrete slabs with and without shear reinforcement. ACI Structural Journal, 2017, 114(4): 875
71. Chou J S, Nguyen N M. Metaheuristics-optimized ensemble system for predicting mechanical strength of reinforced concrete materials. Structural Control and Health Monitoring, 2021, 28(5): e2706
72. Rosen M A, Kishawy H A. Sustainable manufacturing and design: Concepts, practices and needs. Sustainability, 2012, 4(2): 154−174
73. Khishe M, Mosavi M R. Chimp optimization algorithm. Expert Systems with Applications, 2020, 149: 113338
74. Storn R, Price K. Differential evolution—A simple and efficient heuristic for global optimization over continuous spaces. Journal of Global Optimization, 1997, 11(4): 341−359
75. Abdollahzadeh B, Gharehchopogh F S, Mirjalili S. Artificial gorilla troops optimizer: A new nature-inspired metaheuristic algorithm for global optimization problems. International Journal of Intelligent Systems, 2021, 36(10): 5887−5958
76. Abdollahzadeh B, Gharehchopogh F S, Khodadadi N, Mirjalili S. Mountain gazelle optimizer: A new nature-inspired metaheuristic algorithm for global optimization problems. Advances in Engineering Software, 2022, 174: 103282
77. Rao R V, Savsani V J, Vakharia D P. Teaching–learning-based optimization: A novel method for constrained mechanical design optimization problems. Computer Aided Design, 2011, 43(3): 303−315
78. Mirjalili S, Lewis A. The whale optimization algorithm. Advances in Engineering Software, 2016, 95: 51−67
79. Nguyen H D, Truong G T, Shin M. Development of extreme gradient boosting model for prediction of punching shear resistance of R/C interior slabs. Engineering Structures, 2021, 235: 112067